Available online www.jsaer.com

***Journal of Scientific and Engineering Research*, 2023, 10(2):213-229**

Research Article

ISSN: 2394-2630
CODEN(USA): JSERBR

Small Amplitude Ion-Acoustic Compressive and Rarefactive Double Layers in Magnetoplasma Having Cairn's Energy Distribution and Negative Ions

J. K. Chawla[1], P. C. Singhadiya[2]

[1]Govt. Raj Rishi College Alwar, Rajasthan, India-301001
Email: jitendra123chawla@yahoo.co.in
[2]Govt. College Jaipur, Rajasthan, India-302004
Email: prakashsinghadiya82@gmail.com

Abstract Study of ion–acoustic double layers in magnetized plasma with positive and negative ions and nonthermal electrons. The modified Korteweg-de Vries (m-KdV) equation is derived using reductive perturbation method (RPM). The effect of nonthermal electrons, magnetization, obliqueness angle (where obliqueness angle is the angle between wave vector and magnetic field) and negative ions on ion-acoustic compressive and rearafactive double layers are discussed in details. For a given set of parameter values, increases in the magnetization (the obliqueness angle), increases (decreases) the width of the compressive and rarefactive double layer, however the amplitude of the double layers have no effect. The amplitude and width of (Ar^+, F^-), (H^+, H^-) and (H^+, O_2^-) plasmas are discussed in details.

Keywords Magnetoplasma, Cairn's Energy

1. Introduction

The ion-acoustic double layers (IADLs) in magnetized and unmagnetized plasmas have been studied theoretically [1-14] or experimentally [15-20].

Merlino and Loomis [17] has been studied the experimental observation of a strong DLs in a plasma with positive ions, negative ions, and electrons. IADLs have been observed in Solalr flare [21], auroral [22], Jupiter magnetosphere plasmas [23-24].

Several authors [4,5,13] have studied IADLs in different plasma systems by using the RPM. Cairns et al. [25] have been investigated the obliquely propagating ion-acoustic solitons in magnetized plasma with nonthermal electron using the RPM. Bandyopadhyay and Das [6] have been studied the nonlinear behavior of ion acoustic waves in magnetized plasma with nonthermal electrons and found that the amplitude of the DLs increases with the increase in value of nonthermal parameters. Gill et al. [8] investigated the properties of ion-acoustic waves in unmagnetized plasma with nonthermal electron and negative ions using the RPM. They found that for critical value of nonthermal parameter, the DLs are not exist. Das and Bandyopadhyay [10] have been studied obliquely propagating of IADLs in magnetized plasma with nonthermal electron using multiple scale perturbation expansion method. Rios et al. [11] studied the properties of IADLs in a magnetized plasma with nonthermal electron. They found that the amplitude of the DLs decrease with increase the value of nonthermal parameters. Jilani et al. [12] have been studied the ion-acoustic solitons in unmagnetized plasma with pair-ion and non-thermal electron using RPM. They found that effect of the nonthermal electron on characteristic of ion-acoustic soliton. Mishra and Jain [26] have been studied the obliquely propagating ion-acoustic soliton in magnetized plasma with consisting positive and negative ions and nonthermal electrons using the RPM. They found that effect of nontherml electrons on nature of ion-acoustic wave for slow and fast mode. They investigated only ion-acoustic soliton. Here we study the IADLs in magnetized plasma and effect of the nenthermal electron on nature of the double layers.

The IADLs with amplitude were studied in unmagnetized plasmas having nonthermal electron by Gao et al. [14]. Chawla et al. [27] have been studied the ion-acoustic wave in magnetized plasma with nonthermal electrons using the RPM. They study the characteristics (amplitude and width) of the ion-acoustic waves in presence of nonthermal electrons. The amplitude and width of the ion-acoustic waves increases with increase the value of nonthermal parameters.

The layout of this manuscript is organized as follows: In section 2, Using the basic set of hydrodynamic equations governing plasma system and employing RPM and m-KdV equation has been derived. In section 3, the exact solutions of the mKdV equation has been determined. The m-KdV equation has been derived in section 4. Next section is devoted to discussion and the findings. In last section 6, conclusions of our investigations.

2. Basic Equations

We consider collisionless magnetized plasma consisting of warm adiabatic positive and negative ion species and energetic electrons following Cairn's energy distribution with ($T_e >> T_{i1}, T_{i2}$) in a uniform external magnetic field $\vec{B}_0$ along z-axis. We have considered low β plasma. The wave is propagating in the (x-z) plane at an angle θ to the external magnetic field $\vec{B}_0$. The characteristic frequency is assumed to be much smaller as compared to the ion-cyclotron frequency. The dynamics of the plasma is given by the continuity equation, equation of motion and Poisson's equation:

$$\partial_t n_1 + \nabla.(n_1 v_1) = 0 \tag{1}$$

$$\partial_t v_1 + (v_1.\nabla)v_1 = -\frac{1}{\beta}\nabla\phi + \frac{\Omega_{i1}}{\omega_{pi}} v_1 \times \hat{z} - \frac{2\sigma_1}{\beta Z_1}\Delta n_1 \tag{2}$$

$$\partial_t n_2 + \nabla.(n_2 v_2) = 0 \tag{3}$$

$$\partial_t v_2 + (v_2.\nabla)v_2 = \frac{\mu\varepsilon_z}{\beta}\nabla\phi - \frac{\Omega_{i1}}{\omega_{pi}}\mu\varepsilon_z v_2 \times \hat{z} - \frac{2\mu\sigma_2}{\beta Z_1}\Delta n_2 \tag{4}$$

$$\nabla^2\phi = n_e - \frac{n_1}{(1-\alpha\varepsilon_z)} + \frac{\alpha\varepsilon_z}{(1-\alpha\varepsilon_z)} n_2 \tag{5}$$

$$n_e = (1 - \gamma\phi + \gamma\phi^2)e^{\phi} \tag{6}$$

Where,

$$\beta = \frac{(1+\alpha\mu\varepsilon_Z^2)}{(1-\alpha\varepsilon_Z)} \;;\; \alpha = \frac{n_2^{(0)}}{n_1^{(0)}} \;;\; \varepsilon_Z = \frac{Z_2}{Z_1} \;;\; \mu = \frac{M_1}{M_2} \;;\; \sigma_1 = \frac{T_{i1}}{T_e} \;;\; \sigma_2 = \frac{T_{i2}}{T_e} \;;\; \Omega_{i1} = \frac{Z_1 eB_0}{M_1 c};$$

$$\gamma = \frac{4\delta}{(1+3\delta)}$$

In the above equations, n_1, v_1 and n_2, v_2 are the density and fluid velocity of the positive and negative-ion species, respectively, n_{eo} and $n_1^{(0)}$ & $n_2^{(0)}$, are the equilibrium densities of electron components and of the two ion components, respectively. ϕ is the electrostatic potential, μ is the mass ratio of the negative ion species to the positive ion species, α is the equilibrium density ratio of positive to negative ion species, and ε_Z is the charge multiplicity ratio of the negative ion species to positive ion species. The ratio of temperature of positive ion species to the electron temperature is denoted by σ_1 and that of negative ions by σ_2.

In the above equations (1) - (5), velocities (v_1, v_2), potential (ϕ), time (t) and space coordinate (x) have been normalized with respect to ion-acoustic speed in the mixture $C_s = \left[\frac{T_e \beta Z_1}{M_1}\right]^{1/2}$, thermal potential $\frac{T_{eff}}{e}$,

inverse of the ion-plasma frequency in the mixture $\omega_{pi}^{-1}=\left[\frac{4\pi n_e^{(0)}e^2Z_1\beta}{M_1}\right]^{-1/2}$, and Debye length $\lambda_D=\left[\frac{T_e}{4\pi n_e^{(0)}e^2}\right]^{1/2}$.

3. Derivation of The m-KdV Equation

To derive the KdV equation from the basic set of equations, viz., Eqs.(1)-(6), we introduce the following stretching of coordinates (ξ) and (τ) as:

$$\xi=\varepsilon\left(\hat{K}.r-St\right) \tag{7a}$$

And

$$\tau=\varepsilon^3 t \tag{7b}$$

Where ε a small parameter and S is is the phase velocity of the wave, to be determined later. Now we expand the field quantities in the following form:

$$\begin{bmatrix}n_1\\n_2\\v_{1z}\\v_{2z}\\\phi\end{bmatrix}=\begin{bmatrix}1\\1\\0\\0\\0\end{bmatrix}+\varepsilon\begin{bmatrix}n_1^{(1)}\\n_2^{(1)}\\v_{1z}^{(1)}\\v_{2z}^{(1)}\\\phi^{(1)}\end{bmatrix}+\varepsilon^2\begin{bmatrix}n_1^{(2)}\\n_2^{(2)}\\v_{1z}^{(2)}\\v_{2z}^{(2)}\\\phi^{(2)}\end{bmatrix}+\varepsilon^3\begin{bmatrix}n_1^{(3)}\\n_2^{(3)}\\v_{1z}^{(3)}\\v_{2z}^{(3)}\\\phi^{(3)}\end{bmatrix}+\ldots \tag{8a}$$

$$\begin{bmatrix}v_{1\perp}\\v_{2\perp}\end{bmatrix}=\varepsilon^2\begin{bmatrix}v_{1\perp}^{(1)}\\v_{2\perp}^{(1)}\end{bmatrix}+\varepsilon^3\begin{bmatrix}v_{1\perp}^{2}\\v_{2\perp}^{(2)}\end{bmatrix}+\varepsilon^4\begin{bmatrix}v_{1\perp}^{(3)}\\v_{2\perp}^{(3)}\end{bmatrix}+\ldots \tag{8b}$$

Using Eqs. (6), (7) and (8) into Eqs. (1)-(5), we obtain a the lowest-order, i.e., O(ε), one gets the following linear relation

$$\left(\gamma_2+\alpha\mu\varepsilon_Z^2\gamma_1\right)Z_1\cos^2\theta=(1-\gamma)\gamma_1\gamma_2\gamma_3 \tag{9}$$

Here, $\gamma_1=\left(\beta Z_1S^2-2\sigma_1\cos^2\theta\right)$, $\gamma_2=\left(\beta Z_1S^2-2\mu\sigma_2\cos^2\theta\right)$ and $\gamma_3=\left(1-\alpha\varepsilon_Z\right)$

The above equation is quadratic in S^2, therefore inclusion of a finite ion temperature gives rise to two ion-acoustic modes propagating with different phase velocities viz.;

$$S_1^2=\left(\frac{(\mu\sigma_2+\sigma_1)\cos^2\theta}{\beta Z_1}+\frac{\left(1+\alpha\mu\varepsilon_z^2\right)\cos^2\theta}{2(1-\gamma)\beta\gamma_3}\right)-\left[\begin{array}{l}\left(\frac{(\mu\sigma_2+\sigma_1)\cos^2\theta}{\beta Z_1}+\frac{\left(1+\alpha\mu\varepsilon_z^2\right)\cos^2\theta}{2(1-\gamma)\beta\gamma_3}\right)^2\\-\frac{2\mu\cos^4\theta}{\beta^2Z_1^2}\left(\frac{\left(\sigma_2+\alpha\varepsilon_z^2\sigma_1\right)Z_1}{(1-\gamma)\gamma_3}+2\sigma_1\sigma_2\right)\end{array}\right]^{1/2} \tag{10}$$

For the slow ion-acoustic mode, and

$$S_2^2=\left(\frac{(\mu\sigma_2+\sigma_1)\cos^2\theta}{\beta Z_1}+\frac{\left(1+\alpha\mu\varepsilon_z^2\right)\cos^2\theta}{2(1-\gamma)\beta\gamma_3}\right)+\left[\begin{array}{l}\left(\frac{(\mu\sigma_2+\sigma_1)\cos^2\theta}{\beta Z_1}+\frac{\left(1+\alpha\mu\varepsilon_z^2\right)\cos^2\theta}{2(1-\gamma)\beta\gamma_3}\right)^2\\-\frac{2\mu\cos^4\theta}{\beta^2Z_1^2}\left(\frac{\left(\sigma_2+\alpha\varepsilon_z^2\sigma_1\right)Z_1}{(1-\gamma)\gamma_3}+2\sigma_1\sigma_2\right)\end{array}\right]^{1/2} \tag{11}$$

For the fast ion-acoustic mode.

Now taking the next higher order, and using the first-order solutions, we get the second-order solutions. Now the Poisson's equations (5) at O $\left(\varepsilon^2\right)$ gives the following:

$$(1-\gamma)\phi^{(2)}+\frac{1}{2}\phi^{2(1)}-\frac{n_1^{(2)}}{\gamma_3}+\frac{\alpha\varepsilon_Z n_2^{(2)}}{\gamma_3}=0 \tag{12}$$

On substituting the values of $n_1^{(2)}$ and $n_2^{(2)}$ from the second order solutions

$$B\phi^{(1)^2}=0 \tag{13}$$

Where

$$B=\left[\frac{3\beta Z_1 S^2\cos^4\theta}{2\gamma_3}\left\{\frac{Z_1^2}{\gamma_1^{\,3}}-\frac{\alpha\mu^2\varepsilon_z^3}{\gamma_2^{\,3}}\right\}-\frac{1}{2}\right]. \tag{14}$$

therefore $\phi^{(1)}\neq 0$, so "B" should be including in the next order of Poisson's equation. The next higher order, i.e., $O(\varepsilon^3)$ of the Poisson equation on using first and second order solutions gives the following m-KdV equation

$$P\partial_t\phi^{(1)}+B\partial_\xi\phi^{(1)^2}+R\partial_\xi\phi^{(1)^3}+Q\partial_\xi^3\phi^{(1)}=0 \tag{15}$$

$$P=\frac{2\beta Z_1 S\cos^2\theta}{\gamma_3}\left[\frac{Z_1}{\gamma_1^{\,2}}+\frac{\alpha\mu\varepsilon_Z Z_2}{\gamma_2^{\,2}}\right] \tag{16}$$

$$Q=\left[1+\frac{\omega_{pi}^2}{\Omega_{i1}^1}\frac{\beta Z_1^{\,2}S^4\sin^2\theta}{\gamma_1^{\,2}\gamma_3}+\frac{\omega_{pi}^2}{\Omega_{i1}^2}\frac{\alpha}{\mu}\frac{\beta Z_1^{\,2}s^4\sin^2\theta}{\gamma_2^{\,2}\gamma_3}\right] \tag{17}$$

and

$$R=\left[\begin{array}{l}\dfrac{\beta Z_1^{\,4}S^2\cos^6\theta}{\gamma_3\gamma_1^{\,4}}\left\{\dfrac{9\beta Z_1 S^2}{2\gamma_1}-2\right\}\\ +\dfrac{\alpha\mu^3\varepsilon_z^4\beta Z_1 S^2\cos^6\theta}{\gamma_3\gamma_2^{\,4}}\left\{\dfrac{9\beta Z_1 S^2}{2\gamma_2}-2\right\}-\left(\dfrac{1+3\gamma}{6}\right)\end{array}\right] \tag{18}$$

4. Double-layer Solution

For the steady state solution of the mKdV equation (15), we consider

$$\zeta=\xi-u\tau. \tag{19}$$

Where u is a constant velocity.

Using Eq. (19) in Eq. (15) integrating with respect to η, we obtain

$$\frac{1}{2}\left(d_\zeta\phi\right)^2+V(\phi)=0 \tag{20}$$

Where ϕ is used in place of $\phi^{(1)}$ for convenience and $V(\phi)$ is the Sagdeev potential (SP), which is given by

$$V(\phi)=\frac{1}{Q}\left(-\frac{u}{2}P\phi^2+\frac{B}{3}\phi^3+\frac{R}{4}\phi^4\right) \tag{21}$$

In the derivation of Eq. (20) we have used the following boundary conditions.

As $\zeta\to\pm\infty$, ϕ, $d_\zeta\phi$, and $d_\zeta^2\phi\to 0$. The following boundary conditions on the SP should be satisfied

$$V(\phi)=V'(\phi)=0 \text{ at } \phi=0, \tag{22a}$$

$$V(\phi) = V'(\phi) = 0 \text{ at } \phi = \phi_m, \tag{22b}$$

$$V''(\phi) < 0 \text{ at } \phi = 0 \text{ and } \phi_m \tag{22c}$$

Applying boundary conditions (22b) in equation (21), we obtain

$$u = \left(\frac{-R}{2P}\right)\phi_m^2 \tag{23}$$

and

$$\phi_m = -\frac{2}{3}\frac{a}{R} \tag{24}$$

Putting these values in Eq. (21), and obtain

$$V(\phi) = \frac{R\phi^2}{4Q}(\phi_m - \phi)^2 \tag{25}$$

The DLs solution of equation (20), with equation (25), is given by

$$\phi = \frac{\phi_m}{2}\left[1 - \tanh\left\{\left(\frac{-R}{8Q}\right)^{1/2}\phi_m(\xi - u\tau)\right\}\right]. \tag{26}$$

The thickness d of the DLs is given by

$$d = \frac{2\sqrt{\frac{-8Q}{R}}}{|\phi_m|} \tag{27}$$

5. Discussion

To investigate the existence regions and nature of the IADLs in magnetized plasma, we have done numerical calculations for different set of plasma parameters (μ, α, Z_1, Z_2, ε_Z, γ, σ_1, σ_2, θ and ω_{pi}/Ω_i).

In Figure (1a), the variation of the SP $V(\phi)$ with potential (ϕ) for compressive DLs at different value of α with fixed values of other parameters. It is seen that as α increases, the amplitude of the DLs increases. In Fig. (1b), the variation of the SP $V(\phi)$ with potential (ϕ) for compressive DLs at different value of α with fixed values of parameters μ = 0.1 and others are the same as in Figure (1a). It is observed that as α increases, the amplitude of the DLs increases. In Fig. (1c), the variation of the SP $V(\phi)$ with potential (ϕ) for compressive DLs at different value of α with fixed values of parameters μ = 32 and others are the same as in Fig. (1a). It is seen that as α increases, the amplitude of the DLs increases. In Fig. (2a), the variation of the SP $V(\phi)$ with potential (ϕ) for compressive DLs at different value of γ with fixed values of parameters α = 0.6 and others are the same as in Fig. (1a). It is seen that as γ increases, the amplitude of the DLs decreases. In Fig. (2b), the variation of the SP $V(\phi)$ with potential (ϕ) for compressive DLs at different value of γ with fixed values of parameters α = 0.6 and μ = 1 and others are the same as in Fig. (1a). It is seen that as γ increases, the amplitude of the DLs decreases. In Fig. (2c), the variation of the SP $V(\phi)$ with potential (ϕ) for compressive DLs at different value of γ with fixed values of parameters α = 0.01 and μ = 32 and others are the same as in Fig. (1a). It is seen that as γ increases, the amplitude of the DLs increases. In Figure (3a), the variation of the SP $V(\phi)$ with potential (ϕ) for rarefactive DLs at different value of α with fixed values of other parameters. It is seen that as α increases, the amplitude of the DLs decreases. In Fig. (3b), the variation of the SP $V(\phi)$ with potential (ϕ) for rarefactive DLs at different value of α with fixed values of parameters γ =

0.4 and μ = 1 and others are the same as in Fig. (3a). It is seen that as α increases, the amplitude of the DLs decreases. In Fig. (3c), the variation of the SP $V(\phi)$ with potential (ϕ) for rarefactive DLs at different value of α with fixed values of parameters γ = 1.001 and μ = 32 and others are the same as in Fig. (3a). It is seen that as α increases, the amplitude of the DLs increases. In Fig. (4a), the variation of the SP $V(\phi)$ with potential (ϕ) for rarefactive DLs at different value of γ with fixed values of parameters α = 0.4 and others are the same as in Fig. (3a). It is seen that as γ increases, the amplitude of the DLs decreases. In Fig. (4b), the variation of the SP $V(\phi)$ with potential (ϕ) for rarefactive DLs at different value of γ with fixed values of parameters α = 0.29 and μ = 1 and others are the same as in Fig. (3a). It is seen that as γ increases, the amplitude of the soliton decreases. In Fig. (4c), the variation of the SP $V(\phi)$ with potential (ϕ) for rarefactive DLs at different value of γ with fixed values of parameters θ = 32^0, α = 0.0008 and μ = 32 and others are the same as in Fig. (3a). It is seen that as γ increases, the amplitude of the DLs decreases. In Figures (5a) - (5c), 3D curves the variation of ξ, τ and ϕ (equation (26) of the ion-acoustic DLs.

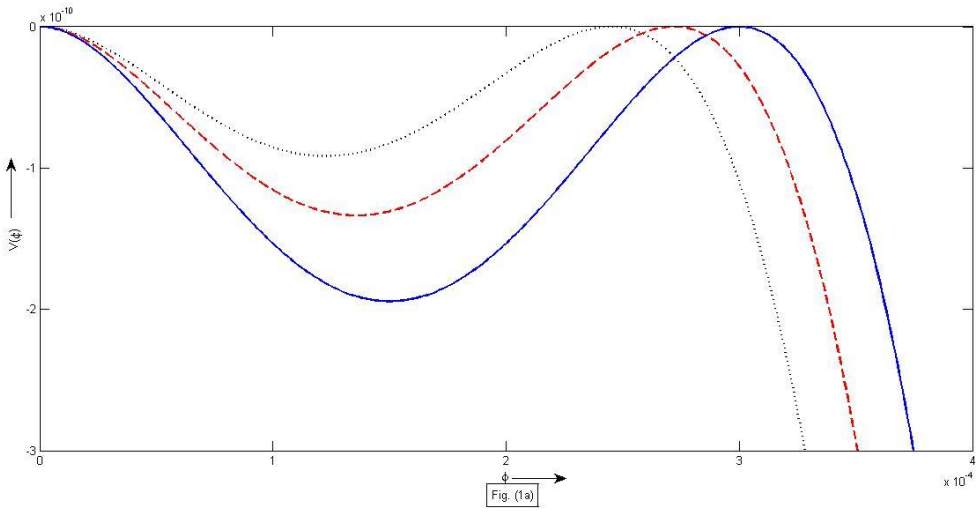

Figure (1a): Variation of the Sagdeev potential $V(\phi)$ *with potential* (ϕ) *of the compressive IADLs for an* (Ar^+, F^-) *plasma with* $\sigma_1 = 0, \sigma_2 = 0.01, Z_1 = 1, Z_2 = 1, \varepsilon_Z = 1,$ $\mu = 0.476,$ $\gamma = 0.01,$ $\theta = 14^0$, *and* $(\omega_{pi} / \Omega_i) = 8$ *at different values of* $\alpha = 0.6$ *(Black color dotted line), 0.63 (red color dashed line) and 0.66 (blue color solid line).*

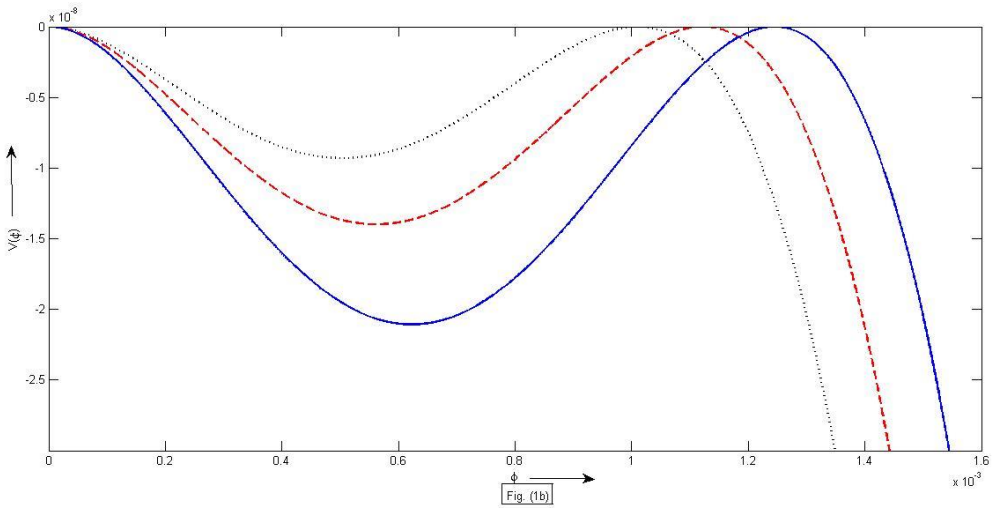

Figure (1b): Variation of the Sagdeev potential $V(\phi)$ *with potential (*ϕ*) of the compressive IADLs for an (H⁺, H⁻) plasma with* $\sigma_1 = 0,\ \sigma_2 = 0.01,\ Z_1 = 1,\ Z_2 = 1,\ \varepsilon_Z = 1,$ $\mu = 1,\ \gamma = 0.01,\ \theta = 14^0$, *and* $(\omega_{pi} / \Omega_i) = 8$ *at different values of* $\alpha = 0.6$ *(black color dotted line), 0.63 (red color dashed line) and 0.66 (blue color solid line).*

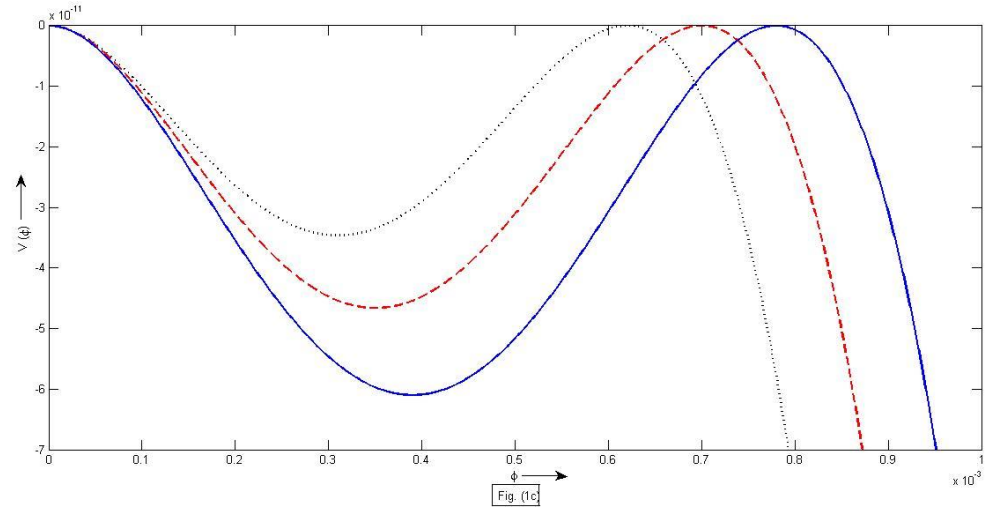

Figure (1c): Variation of the Sagdeev potential $V(\phi)$ *with potential (*ϕ*) of the compressive IADLs for an (H⁺, O₂⁻) plasma with* $\sigma_1 = 0,\ \sigma_2 = 0.01,\ Z_1 = 1,\ Z_2 = 1,\ \varepsilon_Z = 1,$ $\mu = 32,\ \gamma = 0.01,\ \theta = 14^0$, *and* $(\omega_{pi} / \Omega_i) = 8$ *at different values of* $\alpha = 0.01$ *(Black color dotted line), 0.011 (red color dashed line) and 0.012 (blue color solid line).*

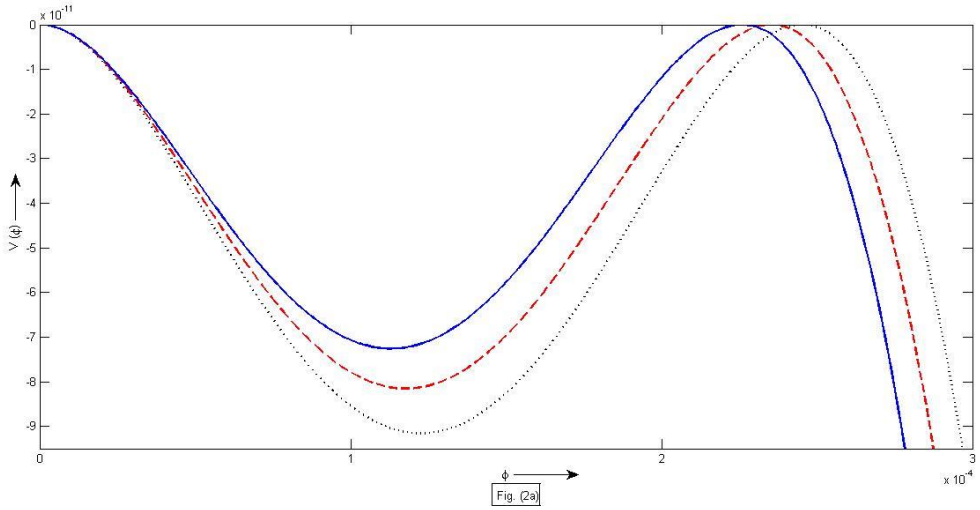

Figure (2a): Variation of the Sagdeev potential $V(\phi)$ *with potential (*ϕ*) of the compressive IADLs for an (Ar*$^+$*, F*$^-$*) plasma with* $\sigma_1 = 0,\ \sigma_2 = 0.01,\ Z_1 = 1,\ Z_2 = 1,\ \varepsilon_Z = 1,$ $\mu = 0.476,\ \alpha = 0.6,\ \theta = 14^0$*, and* $(\omega_{pi} / \Omega_i) = 8$ *at different values of* $\gamma = 0.01$ *(Black color dotted line), 0.012 (red color dashed line) and 0.014 (blue color solid line).*

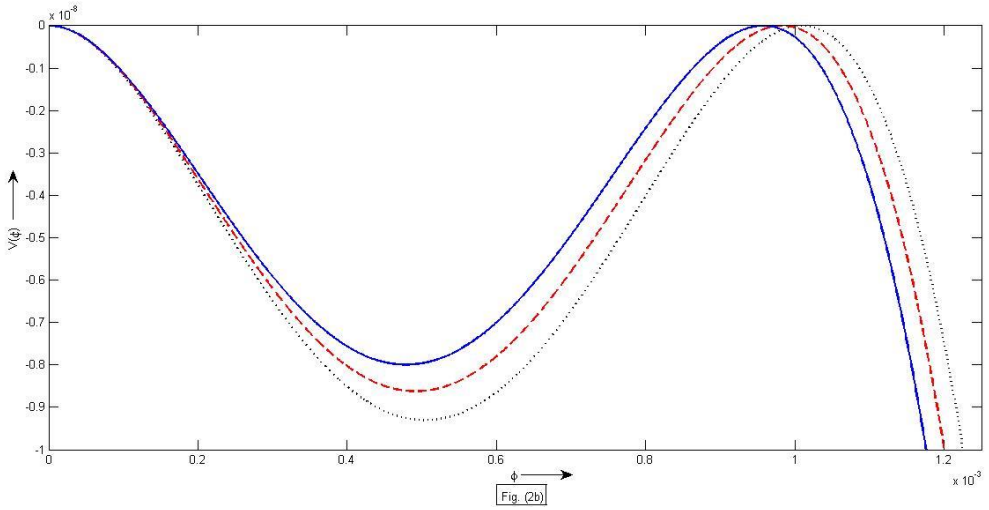

Figure (2b): Variation of the Sagdeev potential $V(\phi)$ *with potential (*ϕ*) of the compressive IADLs for an (H*$^+$*, H*$^-$*) plasma with* $\sigma_1 = 0,\ \sigma_2 = 0.01,\ Z_1 = 1,\ Z_2 = 1,\ \varepsilon_Z = 1,$ $\mu = 1,\ \alpha = 0.6,\ \theta = 14^0$*, and* $(\omega_{pi} / \Omega_i) = 8$ *at different values of* $\gamma = 0.01$ *(Black color dotted line), 0.012 (red color dashed line) and 0.014 (blue color solid line).*

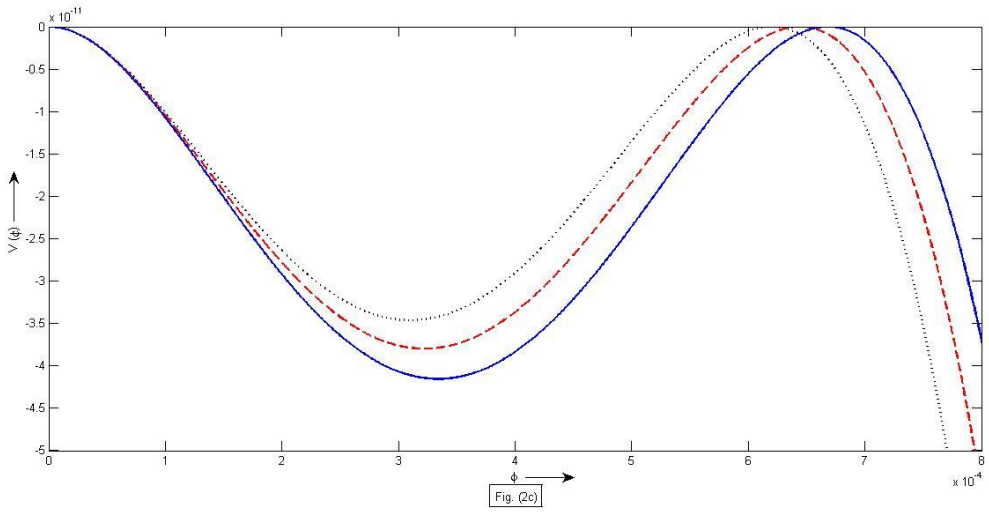

Figure (2c): Variation of the Sagdeev potential $V(\phi)$ *with potential (*ϕ*) of the compressive IADLs for an (H⁺, O₂⁻) plasma with* $\sigma_1 = 0,\ \sigma_2 = 0.01,\ Z_1 = 1,\ Z_2 = 1,\ \varepsilon_Z = 1,$ $\mu = 32,\ \alpha = 0.01,\ \theta = 14^0$, *and* $(\omega_{pi} / \Omega_i) = 8$ *at different values of* $\gamma = 0.01$ *(Black color dotted line), 0.0103 (red color dashed line) and 0.0106 (blue color solid line).*

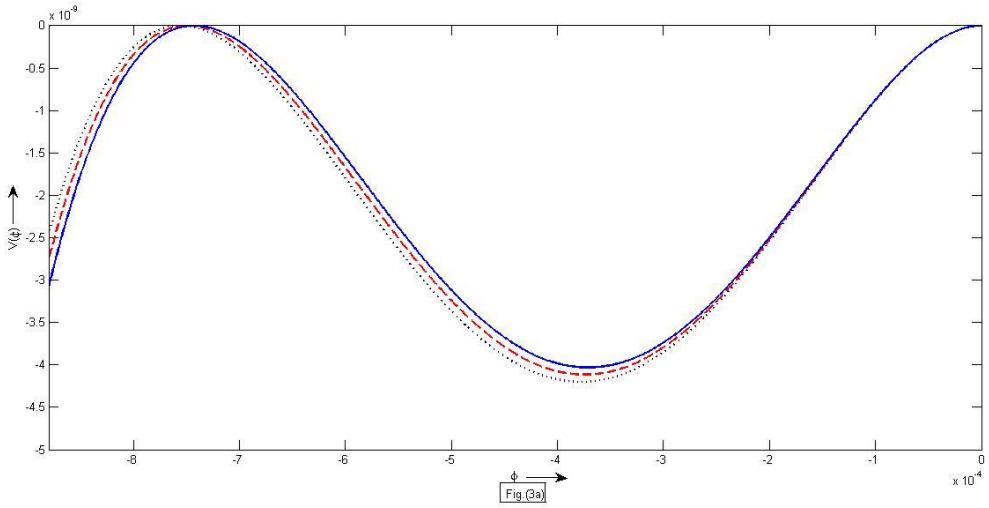

Figure (3a): Variation of the Sagdeev potential $V(\phi)$ *with potential (*ϕ*) of the rarefactive IADLs for an (Ar⁺, F⁻) plasma with* $\sigma_1 = 0.01,\ \sigma_2 = 0,\ Z_1 = 1,\ Z_2 = 1,\ \varepsilon_Z = 1,$ $\mu = 0.476,\ \gamma = 0.5,\ \theta = 15^0$, *and* $(\omega_{pi} / \Omega_i) = 8$ *at different values of* $\alpha = 0.4$ *(Black color dotted line), 0.401 (red color dashed line) and 0.402 (blue color solid line).*

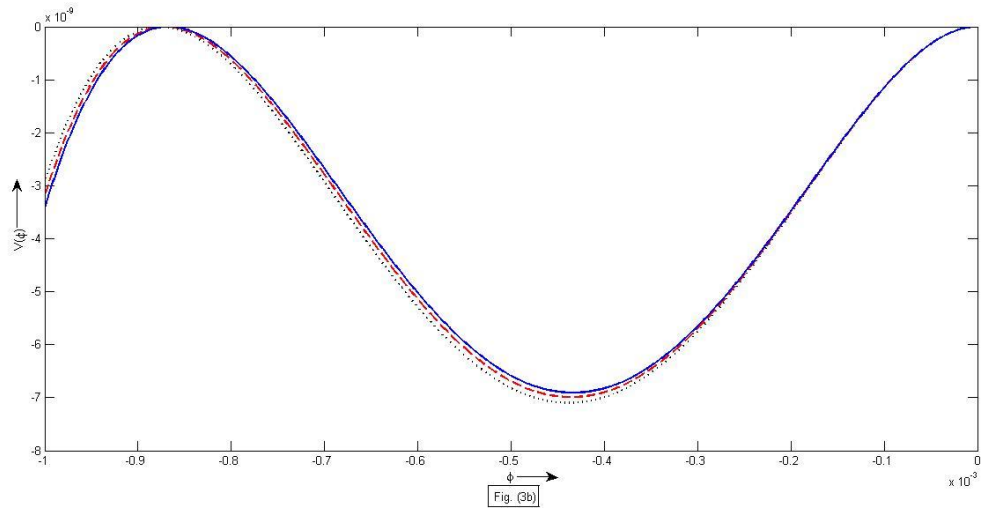

Figure (3b): Variation of the Sagdeev potential $V(\phi)$ *with potential (*ϕ*) of the rarefactive IADLs for an (H⁺, H⁻) plasma with* $\sigma_1 = 0.01,\ \sigma_2 = 0,\ Z_1 = 1,\ Z_2 = 1,\ \varepsilon_Z = 1,$ $\mu = 1,\ \gamma = 0.4,\ \theta = 15^0$, *and* $(\omega_{pi} / \Omega_i) = 8$ *at different values of* $\alpha = 0.29$ *(Black color dotted line), 0.2905 (red color dashed line) and 0.2909 (Blue color solid line).*

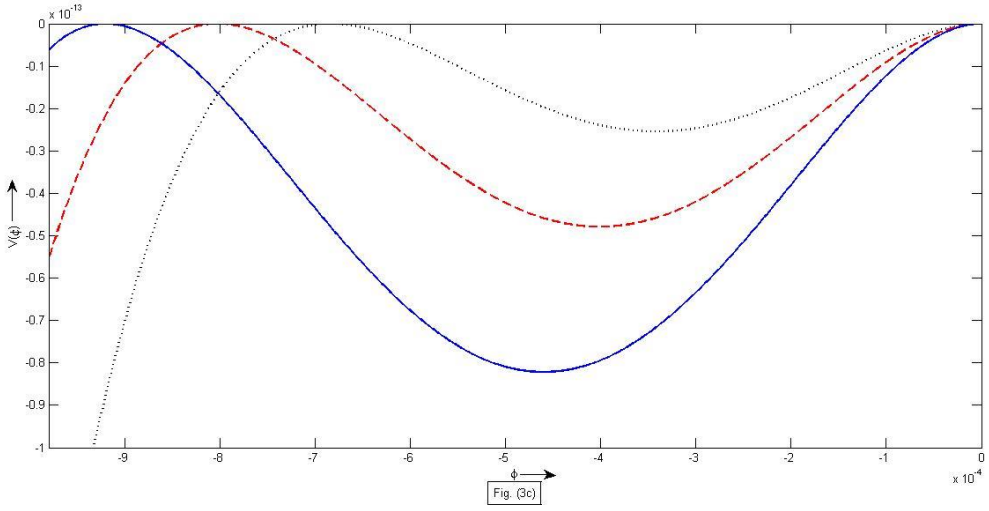

Figure (3c): Variation of the Sagdeev potential $V(\phi)$ *with potential (*ϕ*) of the rarefactive IADLs for an (H⁺, O₂⁻) plasma with* $\sigma_1 = 0.01,\ \sigma_2 = 0,\ Z_1 = 1,\ Z_2 = 1,\ \varepsilon_Z = 1,$ $\mu = 32,\ \gamma = 1.001,\ \theta = 15^0$, *and* $(\omega_{pi} / \Omega_i) = 8$ *at different values of* $\alpha = 0.0008$, *(Black color dotted line), 0.00081 (red color dashed line) and 0.00082 (blue color solid line).*

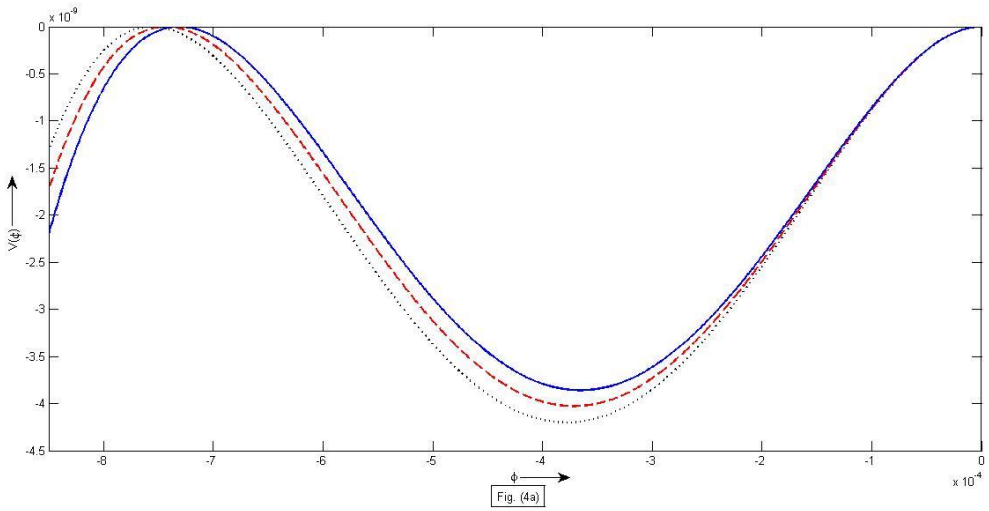

Figure (4a): Variation of the Sagdeev potential $V(\phi)$ *with potential (*ϕ*) of the rarefactive IADLs for an (Ar⁺, F⁻) plasma with* $\sigma_1 = 0.01,\ \sigma_2 = 0,\ Z_1 = 1,\ Z_2 = 1,\ \varepsilon_Z = 1,$ $\mu = 0.476,\ \alpha = 0.4,\ \theta = 15^0$, *and* $(\omega_{pi} / \Omega_i) = 8$ *at different values of* γ *= 0.50 (black color dotted line), 0.501 (red color dashed line) and 0.502 (blue color solid line).*

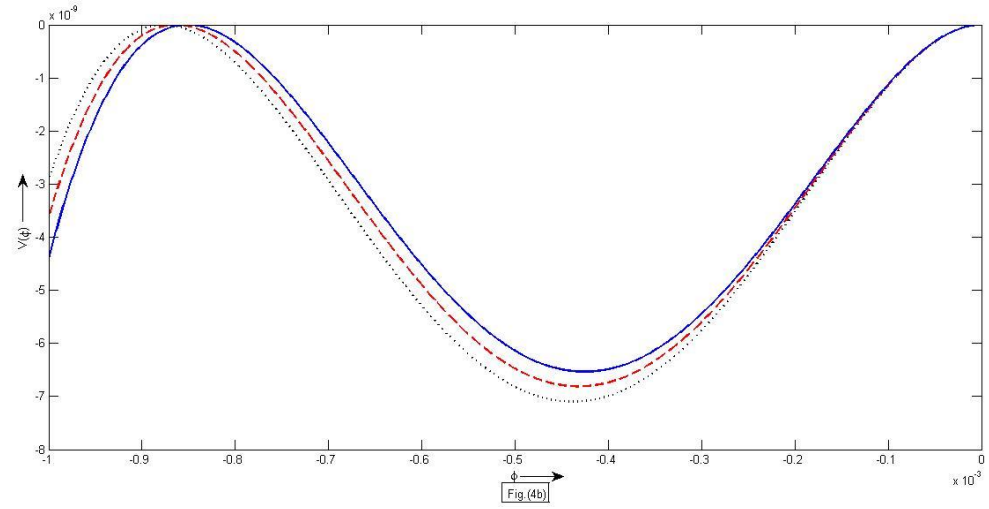

Figure (4b): Variation of the Sagdeev potential $V(\phi)$ *with potential (*ϕ*) of the rarefactive IADLs for an (H⁺, H⁻) plasma with* $\sigma_1 = 0.01,\ \sigma_2 = 0,\ Z_1 = 1,\ Z_2 = 1,\ \varepsilon_Z = 1,$ $\mu = 1,\ \alpha = 0.29,\ \theta = 15^0$, *and* $(\omega_{pi} / \Omega_i) = 8$ *at different values of* γ *= 0.40 (black color dotted line), 0.401 (red color dashed line) and 0.402 (blue color solid line).*

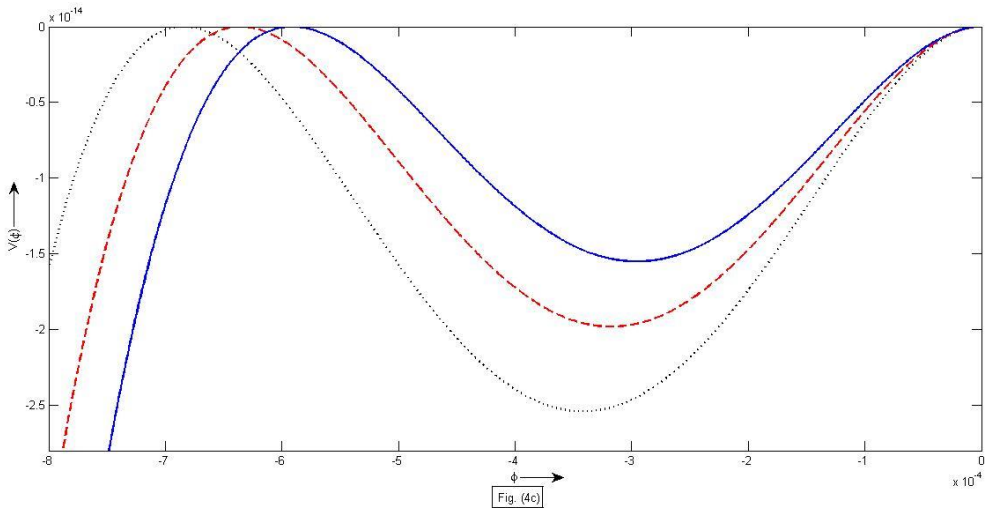

Figure (4c): Variation of the Sagdeev potential $V(\phi)$ *with potential (*ϕ*) of the rarefactive IADLs for an (H⁺, O₂⁻) plasma with* $\sigma_1 = 0.01,\ \sigma_2 = 0,\ Z_1 = 1,\ Z_2 = 1,\ \varepsilon_Z = 1,$ $\mu = 32,\ \alpha = 0.0008,\ \theta = 32^0$, *and* $(\omega_{pi} / \Omega_i) = 8$ *at different values of* γ *= 1.001 (black color dotted line), 1.00103 (red color dashed line) and 1.00106 (Blue color solid line).*

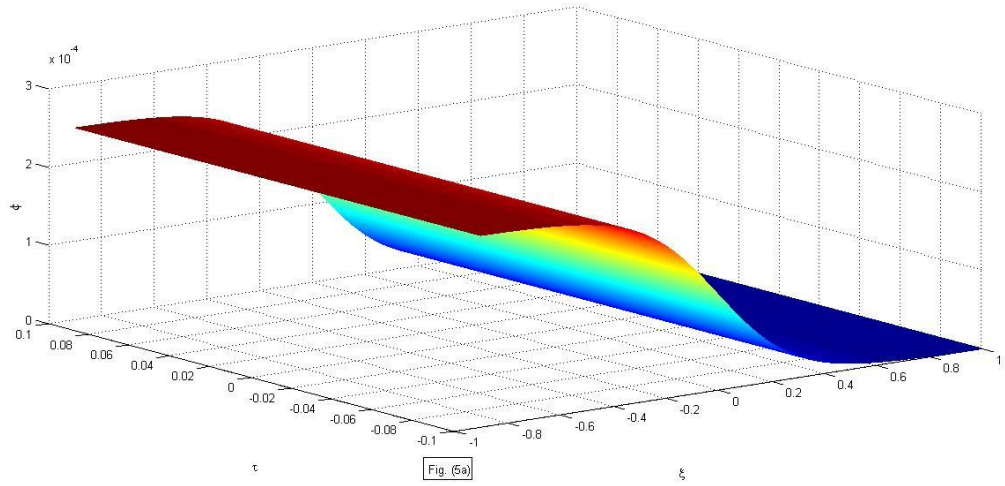

Figure (5a): Variation of ξ, τ *and* ϕ *of the IADLs for an (Ar⁺, F⁻) plasma with* $\sigma_1 = 0,$ $\sigma_2 = 0.01,\ Z_1 = 1,\ Z_2 = 1,\ \varepsilon_Z = 1,\ \mu = 0.476,$ $\gamma = 0.01,\ u = 0.01,\ \alpha = 0.6,$ $\theta = 14^0$, *and* $(\omega_{pi} / \Omega_i) = 8.$

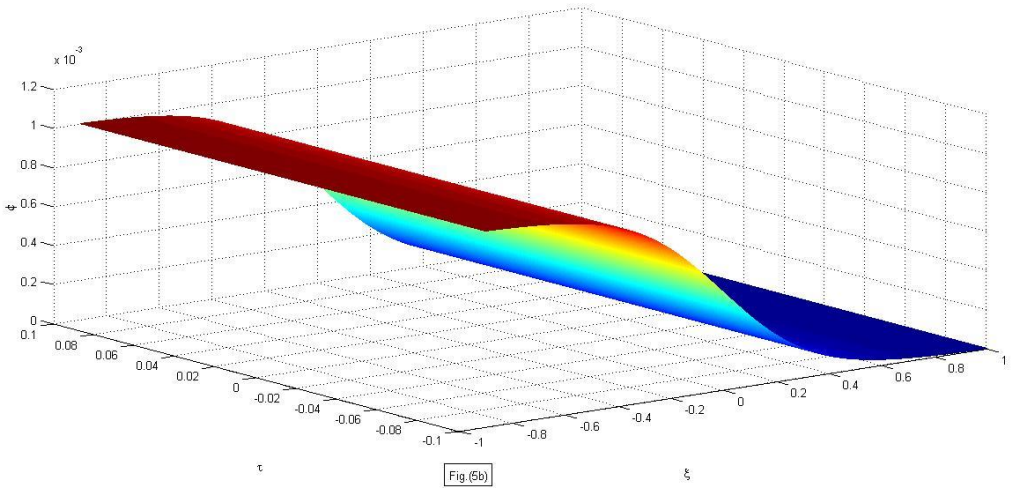

Figure (5b): Variation of ξ, τ *and* ϕ *of the IADLs for an* (H^+, H^-) *plasma with* $\sigma_1 = 0$, $\sigma_2 = 0.01$, $Z_1 = 1$, $Z_2 = 1$, $\varepsilon_Z = 1$, $\mu = 1$, $\gamma = 0.01$, $u = 0.01$, $\alpha = 0.6$, $\theta = 14^0$, *and* $\left(\omega_{pi} / \Omega_i\right) = 8$.

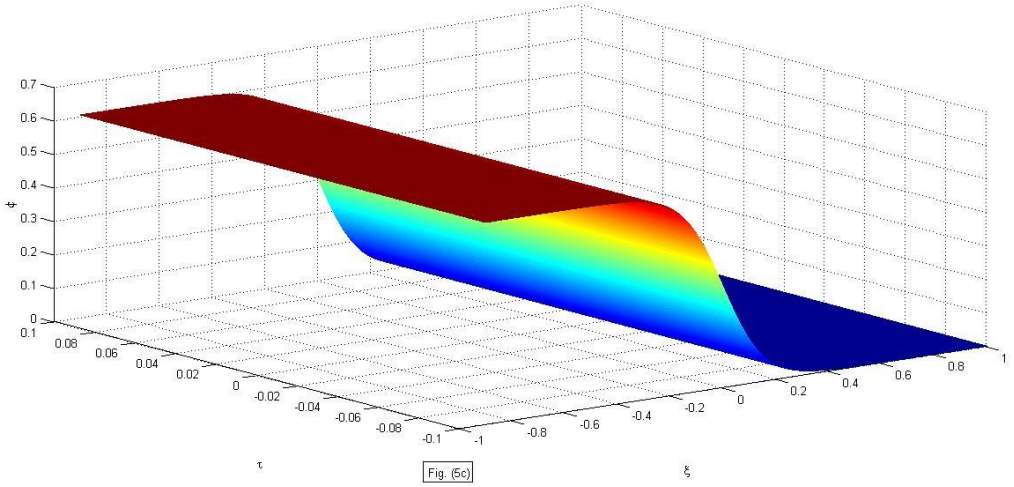

Figure (5c): Variation of ξ, τ *and* ϕ *of the IADLs for an* (H^+, O_2^-) *plasma with* $\sigma_1 = 0$, $\sigma_2 = 0.01$, $Z_1 = 1$, $Z_2 = 1$, $\varepsilon_Z = 1$, $\mu = 32$, $\gamma = 0.01$, $u = 0.01$, $\alpha = 0.3$, $\theta = 14^0$, *and* $\left(\omega_{pi} / \Omega_i\right) = 8$.

Table 1: The amplitude and width of the compressive IADLs for an (Ar^+, F^-) plasma with $\sigma_1 = 0$, $\sigma_2 = 0.01$, $Z_1 = 1$, $Z_2 = 1$, $\varepsilon_Z = 1$, $\mu = 0.476$, $\alpha = 0.6$, $\theta = 14^0$, and $\gamma = 0.01$ at different values of magnetic field (ω_{pi} / Ω_i).

(μ)	Magnetic field	Amplitude	Width
0.476	**8**	**2.452×10^{-4}**	**18.12**
0.476	**9**	**2.452×10^{-4}**	**20.40**
0.476	**10**	**2.452×10^{-4}**	**22.60**

Table 2: The amplitude and width of the compressive IADLs for an (H^+, H^-) plasma with $\sigma_1 = 0$, $\sigma_2 = 0.01$, $Z_1 = 1$, $Z_2 = 1$, $\varepsilon_Z = 1$, $\mu = 1$, $\alpha = 0.6$, $\theta = 14^0$, and $\gamma = 0.01$ at different values of magnetic field (ω_{pi} / Ω_i).

(μ)	Magnetic field	Amplitude	Width
1	8	1.009×10^{-3}	7.40
1	9	1.009×10^{-3}	8.35
1	10	1.009×10^{-3}	9.30

Table 3: The amplitude and width of the compressive IADLs for an (H^+, O_2^-) plasma with $\sigma_1 = 0$, $\sigma_2 = 0.01$, $Z_1 = 1$, $Z_2 = 1$, $\varepsilon_Z = 1$, $\mu = 32$, $\alpha = 0.01$, $\theta = 14^0$, and $\gamma = 0.01$ at different values of magnetic field (ω_{pi} / Ω_i).

(μ)	Magnetic field	Amplitude	Width
32	8	6.21×10^{-4}	74.50
32	9	6.21×10^{-4}	83.80
32	10	6.21×10^{-4}	93.70

Table 4: The amplitude and width of the rarefactive IADLs for an (Ar^+, F^-) plasma with $\sigma_1 = 0.01$, $\sigma_2 = 0$, $Z_1 = 1$, $Z_2 = 1$, $\varepsilon_Z = 1$, $\mu = 0.476$, $\alpha = 0.4$, $\theta = 15^0$, and γ = 0.5 at different values of magnetic field (ω_{pi} / Ω_i).

(μ)	Magnetic field	Amplitude	Width
0.476	8	7.53×10^{-4}	8.248
0.476	9	7.53×10^{-4}	9.28
0.476	10	7.53×10^{-4}	10.25

Table 5: The amplitude and width of the rarefactive IADLs for an (H^+, H^-) plasma with $\sigma_1 = 0.01$, $\sigma_2 = 0$, $Z_1 = 1$, $Z_2 = 1$, $\varepsilon_Z = 1$, $\mu = 1$, $\alpha = 0.29$, $\theta = 15^0$, and γ = 0.40 at different values of magnetic field (ω_{pi} / Ω_i).

(μ)	Magnetic field	Amplitude	Width
1	8	8.768×10^{-4}	7.357
1	9	8.768×10^{-4}	8.25
1	10	8.768×10^{-4}	9.30

Table 6: The amplitude and width of the rarefactive IADLs for an (H^+, O_2^-) plasma with $\sigma_1 = 0.01,\ \sigma_2 = 0,\ Z_1 = 1,\ Z_2 = 1,\ \varepsilon_Z = 1,\ \mu = 32,\ \alpha = 0.0008,\ \theta = 15^0$, and γ = 1.001 at different values of magnetic field (ω_{pi} / Ω_i).

(μ)	Magnetic field	Amplitude	Width
32	8	6.84×10^{-4}	3040
32	9	6.84×10^{-4}	3400
32	10	6.84×10^{-4}	3750

Table 7: The amplitude and width of the compressive ion acoustic double layers at different values of obliqueness (θ) with fixed value of $(\omega_{pi} / \Omega_i) = 8$ and others are same as in Table1.

(μ)	Obliqueness (θ)	Amplitude	Width
0.476	14.0^0	2.452×10^{-4}	18.12
0.476	14.5^0	2.452×10^{-4}	17.15
0.476	14.9^0	2.452×10^{-4}	13.30

Table 8: The amplitude and width of the compressive IADLs for an (H^+, H^-) plasma with at different values of obliqueness (θ) with fixed value of $\mu = 1$ and $(\omega_{pi} / \Omega_i) = 8$ and others are same as in Table1.

(μ)	Obliqueness (θ)	Amplitude	Width
1	14.0^0	1.009×10^{-3}	7.40
1	14.5^0	1.009×10^{-3}	6.98
1	14.9^0	1.009×10^{-3}	5.48

Table 9: The amplitude and width of the compressive IADLs for an (H^+, O_2^-) plasma at different values of obliqueness (θ) with fixed value of $\mu = 32$ and $(\omega_{pi} / \Omega_i) = 8$ and others are same as in Table1.

(μ)	Obliqueness (θ)	Amplitude	Width
32	14.0^0	6.21×10^{-4}	74.50
32	14.5^0	6.21×10^{-4}	70.50
32	14.9^0	6.21×10^{-4}	54.98

Table 10: The amplitude and width of the rarefactive ion acoustic double layers at different values of obliqueness (θ) with fixed value of $(\omega_{pi} / \Omega_i) = 8$ and others are same as in Table 4.

(μ)	Obliqueness (θ)	Amplitude	Width
0.476	15.00	7.53×10^{-4}	8.248
0.476	15.1^0	7.53×10^{-4}	7.28
0.476	15.2^0	7.53×10^{-4}	6.20

Table 11: The amplitude and width of the rarefactive ion acoustic double layers at different values of obliqueness (θ) with fixed value of $(\omega_{pi} / \Omega_i) = 8$ and others are same as in Table 5.

(μ)	Obliqueness (θ)	Amplitude	Width
1	15.0^0	8.768×10^{-4}	7.357
1	15.1^0	8.768×10^{-4}	6.48
1	15.2^0	8.768×10^{-4}	5.50

Table 12: The amplitude and width of the rarefactive ion acoustic double layers at different values of obliqueness (θ) with fixed value of $(\omega_{pi}/\Omega_i)=8$ and others are same as in Table 6.

(μ)	Obliqueness (θ)	Amplitude	Width
32	15.0^0	6.84×10^{-4}	3040
32	15.1^0	6.84×10^{-4}	2700
32	15.2^0	6.84×10^{-4}	2300

6. Conclusion

We have studied obliquely propagating of ion-acoustic compressive and rarefactive DLs in magnetized plasma consisting of positive and negative ions, and nonthermal electrons with using the RPM and derive the mKdV equation. Our main conclusions of this manuscript are given below:

(1) An increase the magnetization, the width of the ion-acoustic compressive and rarefactive double layer increases shown in Table 1- Table 6.
(2) The angle of obliqueness (θ) increases, the width of the ion-acoustic compressive and rarefactive Dls decreases shown in Table 7- Table 12.
(3) The angle of obliqueness and magnetization does not affect the amplitude of the ion-acoustic compressive and rarefactive DLs shown in Table 1- Table 12.
(4) For a given set of parameters, it is found that the amplitudes and width of ion-acoustic compressive (rarefactive) DLs increases (decreases) with increasing negative ion concentration.
(5) For a given set of parameters, it is found that the amplitudes and width of ion-acoustic compressive (rarefactive) DLs decreases with increasing nonthermal electron parameter.

For a given set of parameters, it is found that the amplitudes and width of ion-acoustic compressive (rarefactive) double layer increases with increasing nonthermal electron parameter (negative ion concentration) only for (H^+, O_2^-) plasmas shown in Fig. (2c) and (3c) respectively.

References

[1]. L. P. Block, Astrophys. Space Sci. 55, 59 (1978).
[2]. H. Schamel, Phys. Scr. T2/1, 228 (1982).
[3]. M. A. Raadu, Phys. Rep. 178, 25 (1989).
[4]. S. L. Jain, R. S. Tiwari and S. R. Sharma, Can. J. Phys. 68, 474 (1990).
[5]. L. L. Yadav and S. R. Sharma, Phys. Scr. 43, 106 (1991).
[6]. A. Bandyopadhyay and K. P. Das, Physics Scripta 61, 92 (2000).
[7]. M. K. Mishra, A. K. Arora and R. S. Chhabra, Phys. Rev. E 66, 16402 (2002).
[8]. T. S. Gill, P. Bala, H. Kaur, N. S. Saini, S. Bansal and J. Kaur, Eur. Phys. J. D 31, 91 (2004).
[9]. M. K. Mishra, R. S. Tiwari and S. K. Jain, Phys. Rev. E 76, 036401 (2007).
[10]. J. Das and A. Bandyopadhyay, J. Plasma Physics 74, 163 (2008).
[11]. L. A. Rios and R. M. O. Galvão, Physics Plasmas 20, 112301 (2013).
[12]. K. Jilani, A. M. Mirza and T. A. Khan, Astrophys Space Sci 344, 135 (2013).
[13]. J. K. Chawla and M. K. Mishra, Astrophys Space Sci 343, 629 (2013).
[14]. D. N. Gao, J. Zhang, Y. Yang and W. S. Duan, Plasma Physics Reports (2017) DOI: 10.1134/S1063780X17080062.
[15]. A. N. Sekar and Y.C. Saxena, Plasma Phys. Controlled Fusion 27, 181 (1985).
[16]. N. Hershkowitz, Space Sci. Rev. 41, 351 (1985).
[17]. R. L. Merlino and J. J. Loomis, Phys. Fluids B 2, 2865 (1990).
[18]. H. Hairapetian and R. L. Stenzel, Phys. Rev. Lett. 65, 175 (1990).
[19]. J. L. Ferreira, G. O. Ludwig and A. Montes, Plasma Phys. Control. Fusion 33, 297 (1991).
[20]. N. Plihon and P. Chabert, Physics Plasmas 18, 082102 (2011).
[21]. H. Alfven and P. Carlqvist, Sol. Phys. 1, 220 (1967).
[22]. M. Temerin, K. Cerny, W. Lotko and F. S. Mozer, Phys. Rev. Lett. 48, 1175 (1982).
[23]. D. D. Sentman and C. K. Goertz, JPR Space Physics 83, 3151 (1978).

[24]. R. Boström, G. Gustafsson, B. Holback, G. Holmgren, H. Koskinen and P. Kitner, Phys. Rev. Lett. 61, 82 (1988).
[25]. R. A. Crains, A. A. Mamun, R. Bingham and P. K. Shukla, Physica Scripta. T63, 80 (1996).
[26]. M. K. Mishra and S. K. Jain, J. Plasma Physics 79, 893 (2013).
[27]. J. K. Chawla, P. C. Singhadiya and R. S. Tiwari, Pramana J. Phys. 94, 13 (2020).